Overview of progress in establishing the plasma basis of STEP

H Meyer[1], F Casson[2], N Conway[2], S Freethy[2], T Hender[2], M Henderson[1], S Henderson[2], K Kirov[2], M Lennholm[2], K McClements[2], J Morris[2], C Roach[2], S Saarelma[2], D Valcarel[2], the STEP Plasma Team

[1]*UK Industrial Fusion Solutions Ltd, Culham Campus, Abingdon OX14 3DB, UK*

[2]*UKAEA, Culham Campus, Abingdon OX14 3DB, UK*

The UK's Spherical Tokamak for Energy Production (STEP) programme is developing conceptual designs for a prototype magnetic confinement fusion power plant, targeting 2040. Central to the design is a fully non-inductive plasma solution [1] and a robust control system [2]. External heating and current drive (CD) are microwave-based, with both pure electron cyclotron CD (ECCD) and a mix of on-axis ECCD and off-axis electron Bernstein wave CD (EBWCD) in the designs [3]. EBWCD is projected to have normalised current drive efficiency up to three times higher than ECCD, providing possible access to a $Q_{\rm fus} = P_{\rm fus}/P_{\rm aux} \sim 30$ flat-top operating point (FTOP): this compares to $Q_{\rm fus}\sim 11$ needed for net electricity output of $P_{\rm net}\sim 100$ MW [1]. The published design point (SPP-1) [1], with geometric major radius $R_{\rm geo} = 3.6$ m, aspect ratio $A = 1.8$ and toroidal field $B_t(R_{\rm geo}) = 3.2$ T, generating fusion power $P_{\rm fus}\sim 1.5 - 1.8$ GW, has been found to be technically challenging due to constraints on the inner build radius. This has led to a pivot to a larger design (SPP-2) with $R_{\rm geo} = 4.3$ m but the same A and $P_{\rm fus}$, while options to maintain a smaller design point continue to be explored.

Due to limited space in the centre column, only a small solenoid will be used, specifically for driving the plasma current I_p during the early ramp-up phase to ~2MA. ECCD (fundamental then 2nd harmonic O-mode) will be used to ramp-up the current from ~2MA to the flat-top value ~20MA. During this non-inductive phase the plasma density will be kept low to optimize the ECCD efficiency $\eta_{\rm CD} \sim T_e/n_e$ [3]. The required ECCD power (~150 MW) is determined by an assumed quality of confinement as well as $\eta_{\rm CD}$. The transport is assumed to be Bohm/gyro-Bohm in character. When the full I_p has been reached, the density is

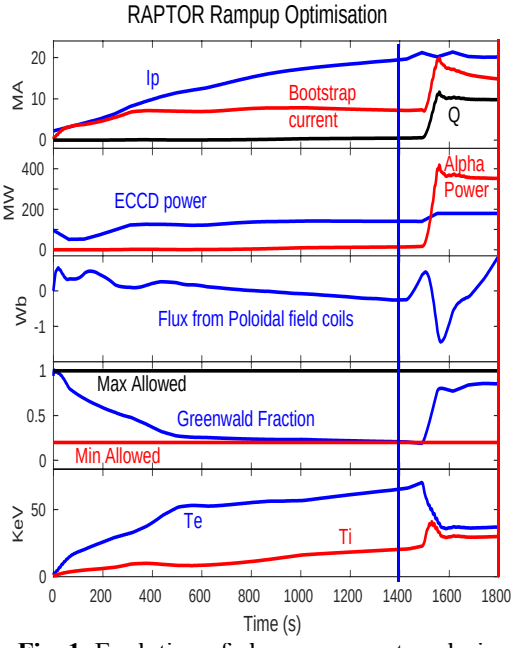

Fig. 1. Evolution of plasma parameters during ramp-up of SPP-1 computed using RAPTOR [4].

raised to achieve fusion burn conditions $Q_{\mathrm{fus}} \approx 10$ with high bootstrap fraction. The RAPTOR code is being used to optimize the ramp-up scenario, subject to a number of constraints listed below (Fig. 1), and has also been used for burn control modelling [4].

For the flat-top, in the absence of validated and sufficiently fast predictive transport models, the confinement quality is again assumed, with Bohm/gyro-Bohm transport scaled to achieve P_{fus} in the range 1.5-1.8 GW [5]. The scenario space is then constrained by 6 other conditions, including $Q_{\mathrm{fus}} \geq 11$, $I_p \leq 25\mathrm{MA}$, $P_{\mathrm{sep}}/R_{\mathrm{geo}} \leq 45\mathrm{MWm}^{-1}$ (P_{sep} is the power crossing the separatrix). As shown in Fig. 2, regions of scenario space in SPP-1 satisfying most of these constraints are narrow when pure ECCD is used even if optimistic confinement is assumed ($H_{\mathrm{IPB98(y,2)}} < 1.4$). Adding EBWCD and reducing the core radiation fraction f_{rad}^{core} widens the operating space that satisfies most of the constraints [4].

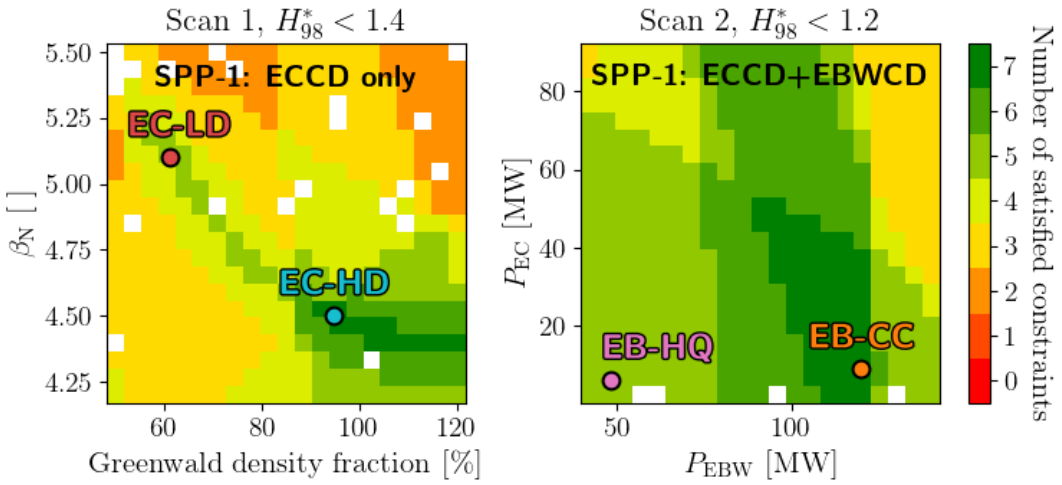

Fig. 2. Number of constraints simultaneously satisfied versus β_N and Greenwald density fraction in pure ECCD operating points (left plot), and versus ECCD power and EBWCD power in operating points that employ both types of microwave current drive (right plot).

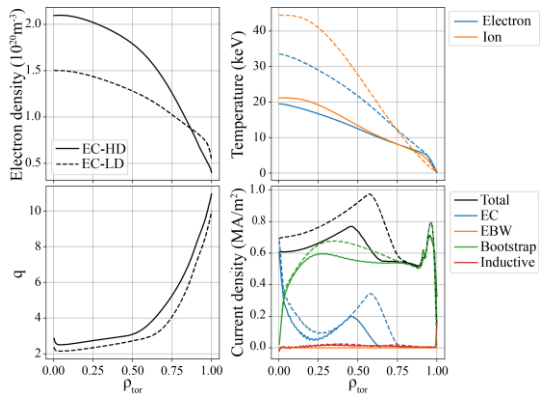

Parameter	EC-HD	EC-LD
f_{rad}^{core}	0.7 (He, Ar, Xe)	
I_p [MA], f_{BS}	21, 0.9	25, 0.8
P_{fus} [GW]	1.68	1.51
Q	11.1	9.2
P_{net}^{el} [MW]	115	37
P_{EC}, P_{EBW}[MW]	150, 0	160, 0
$f_{GW} = \bar{n}_e/n_{GW}$	0.95	0.61
β_N	4.5	5.1
$l_i(3)$	0.3	0.3
τ_E [s]	4.2	5.4
P_{sep}/R_{geo} [MW/m]	39	40
$(H + H^*)/2$	1.4[1] 1.4[2]	1.8[1] 1.4[2]

Fig. 3. Left: profiles of 1D plasma parameters in high (solid curves) and low (dashed curves) density SPP-1 operating points with pure ECCD external current drive. Right: 0D parameters in these operating points. Here, $\ell_i(3)$ is normalized internal inductance and H^* is a confinement factor corrected for highly-radiating plasmas.

The SOLPS-ITER code has been used to determine the optimum divertor geometry and seed gas fuelling conditions for detachment of the exhaust plasma, corresponding to target ion temperature $T_{i,t} < 5$eV [6]. Partial inner target detachment is always achieved at lower D and Ar gas puff than outer target detachment (Fig 4a) while pronounced inner detachment is only achieved with horizontal or X-divertor geometries (Fig 4b). The X-divertor provides the optimum balance between the requirements of detachment and neutral trapping/pumping.

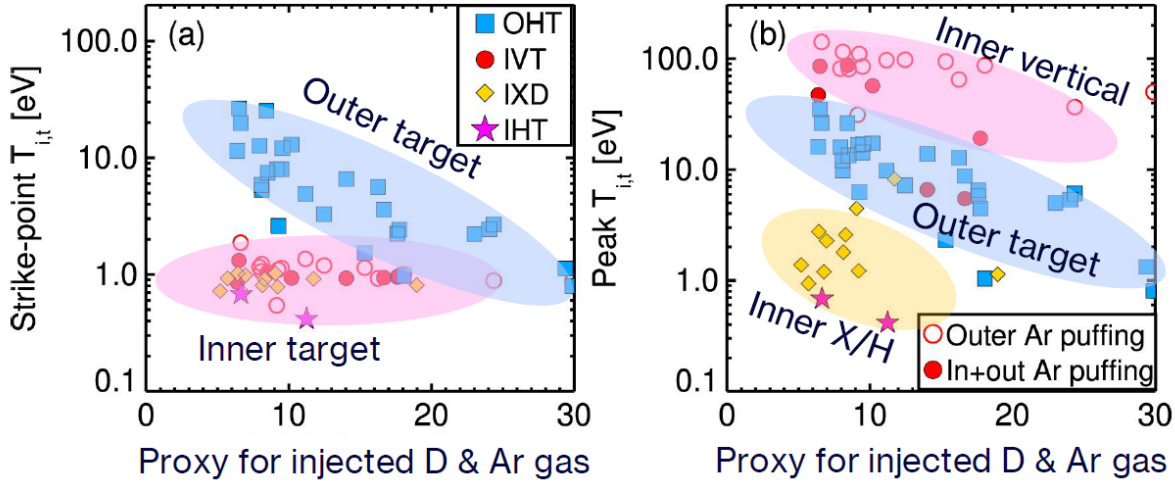

Fig. 4. Left: SOLPS-ITER calculations of (a) strike-point ion temperature and (b) peak target ion temperature versus a proxy for the D and Ar injection rate in several divertor configurations (outer horizontal target, inner vertical target, inner X-point divertor, inner horizontal target), and for outer-only Ar puffing (unfilled symbols) and a mixture of inner and outer Ar puffing (filled symbols). The coloured ovals are present to guide the eye.

The advantage of EBWCD relative to ECCD is lost in SPP-2: typically in SPP-1 $\eta_{\mathrm{EBW}} \approx 2\eta_{\mathrm{EC}}$ off-axis whereas in SPP-2 $\eta_{\mathrm{EBW}} \leq \eta_{\mathrm{EC}}$ across the plasma (Fig. 5), due mainly to a fall in pedestal temperature. Requiring $f_{GW} \leq 1.0$ in a higher minor radius device with similar I_p leads to lower density and hence increased ECCD efficiency. The SPP-2 profiles, which determine the current drive efficiencies, are also informed by modified transport coefficients based on nonlinear gyrokinetic simulations.

The baseline SPP-2 design has 12 picture-frame toroidal field (TF) coils. Simulating TF ripple-induced fusion α-particle losses using the LOCUST code, we have found that the losses are acceptable if the TF coil outer limbs are located at major radius $R_{\mathrm{coil}} \geq 10.5$m. SPP-1 and SPP-2 have been designed with several sets of control coils, including ELM suppression coils. LOCUST simulations show that α-particle losses from SPP-1 due to 3D fields arising from ELM coils depend strongly on the phase shift $\Delta\phi$ between the currents in coils above and below the midplane, indicating that $\Delta\phi$ needs to be optimised for both ELM suppression and α-particle confinement (Fig. 6, left). Since SPP-1 would need to operate at β_N above the no-wall stability

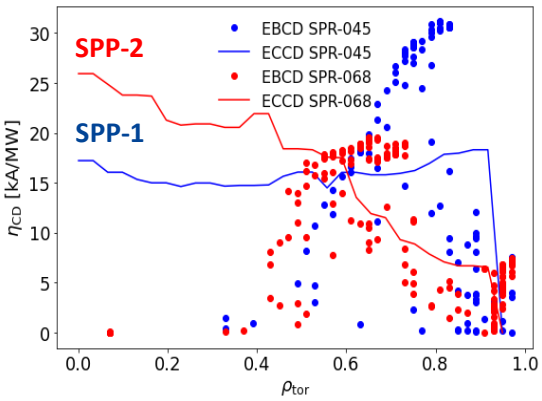

Fig. 5. Current drive efficiency profiles for ECCD (solid curves) and EBWCD (circles) in SPP-1 (blue) and SPP-2 (red).

limit for resistive wall modes (RWMs) with toroidal mode number $n = 1$, passive and active control of these modes will be needed [7]. When sensor noise is present, controlled RWMs saturate at finite amplitude and cause additional α-particle losses: however, these losses are negligible at sub-disruption mode amplitudes, $\delta B \leq 0.01$T. The stability of toroidal Alfvén eigenmodes (TAEs) has been modelled using the HALO wave-particle interaction code [8]. TAEs have been found to be suppressed in the SPP-1 and SPP-2 flat-tops by fuel ion Landau damping, due to its strong (exponential) dependence on fuel ion β, despite strong α-particle drive (Fig. 6, right). However, these modes could still be excited by energetic electrons arising from ECCD during ramp-up when fuel ions are cool due to resonance with electrons close to the trapped/passing boundary.

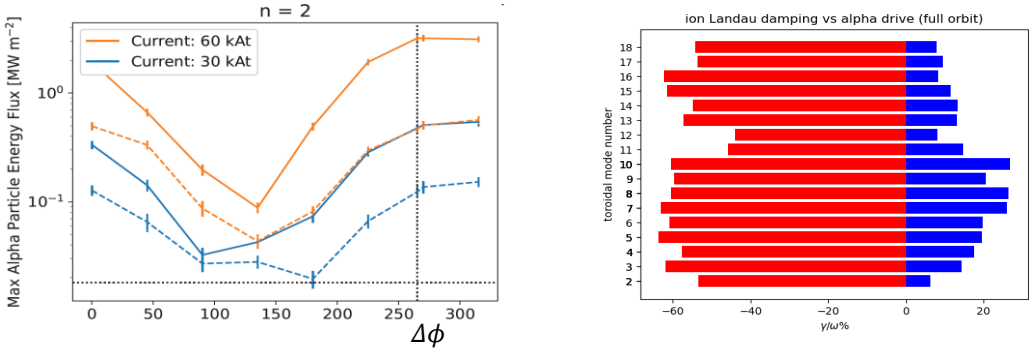

Fig. 6. Left: maximum α-particle power loading on 1st wall due to $n = 2$ ELM coil perturbations in SPP-1 versus $\Delta\phi$ with (solid curves) and without (dashed curves) the plasma response included. Right: TAE growth (blue) and Landau damping (red) rates in SPP-2.

In summary, possible ramp-up paths via ECCD to burning plasma conditions in STEP have been identified, while EBWCD widens the operational space that satisfies most of the requirements of a reactor in the flat-top. Inner X-point targets have been found to provide the optimum divertor configuration, and TAEs are stable in the flat-top due to ion Landau damping.

[1] H Meyer Phil. Trans. R. Soc. A **382**, 20230406 (2024); [2] M Lennholm et al. Phil. Trans. R. Soc. A **382**, 20230403 (2024); [3] S Freethy et al. Nucl. Fusion **64**, 126035 (2024) ; [4] J Mitchell et al. Fusion Engineering & Design **219**, 115202 (2025); [5] E Tholerus et al. Nucl. Fusion **64**, 106030 (2024); [6] SS Henderson et al. Nucl. Fusion **65**, 016033 (2025); [7] G Xia et al. Nucl. Fusion 63, 026021 (2023); [8] M Fitzgerald et al. Computer Physics Communications **252**, 106773 (2020)